Analysis of stochastic resonances

Petr Chvosta*
Department of Macromolecular Physics, Faculty of Mathematics and Physics, Charles University, V Holešovičkách 2, CZ-180 00 Praha, Czech Republic

Peter Reineker†
Abteilung Theoretische Physik, Universität Ulm, Albert-Einstein-Allee 11, 89069 Ulm, Germany
(Received 22 June 2003; revised manuscript received 4 September 2003; published 18 December 2003)

We investigate the one-dimensional diffusion of a particle in a piecewise linear potential superimposed with a step of a harmonically modulated height. Employing the matching conditions, we solve the corresponding Fokker-Planck equation and we analyze nonlinear features of the particle's mean position as a function of time. We present detailed results in two physically relevant cases. First, we take the unperturbed potential as a symmetrical up-oriented tip, which is placed between two reflecting boundaries and we add the jump at the tip coordinate. The setting yields resonancelike behavior of the stationary-response amplitude. Second, if the discontinuity at origin is combined with the constant force in the symmetrical region between the boundaries, the stationary response displays a time-independent shift against the potential slope. The driving-induced force exhibits a resonance-like behavior both with respect to the diffusion constant and the slope of the unperturbed potential.

DOI: 10.1103/PhysRevE.68.066109 PACS number(s): 02.50.Ey, 05.10.Gg, 05.40.−a, 05.40.Jc

I. INTRODUCTION

The dynamical behavior of an overdamped Brownian particle acted upon by the thermal force and moving in a fixed potential landscape is a well understood classical problem [1–3]. However, in the last decade, the diffusion dynamics has been reexamined in systems in which the potential depends on time, the modulation being due to additional (deterministic [4] and/or stochastic [5]) dynamical mechanisms [6]. The new achievements have substantially broadened the field. References [7,8] are two of the recent reviews which discuss history, applications, and existing literature within the domain.

In a paradigmatic setting, consider a particle which diffuses in a potential profile and which is additionally acted upon by a harmonically oscillating force. Then the whole potential landscape changes in time and the corresponding dynamical equation cannot be solved in closed form. One has to invoke an appropriate approximation which typically assumes a separation of time scales. However, the most interesting phenomena within this domain are just based on time-scale matching conditions and their description requires a nonperturbational approach. Any exactly solvable diffusion model with a time-dependent potential is of a considerable value even if it is only as a test of existing approximative treatments.

In the present paper, we have two objectives. First, on the methodological side, we want to examine a different approach, which allows for a detailed analysis of a broad class of diffusion problems with time-dependent potentials. In this approach, the price paid for the exact solutions is a simplified implementation of the external driving. We assume that the time-dependent perturbation influences the original potential just within a very narrow region around a given point. In brief, we add a step with time-dependent height. It will be shown that such a device still keeps all the pertinent aspects of the diffusion dynamics. The results are valid for any form of time-dependent function which controls the step height (this function represents the input signal).

Our second objective is the detailed analysis of two physically relevant problems. First, we assume a symmetric double-well unperturbed potential. Adding a harmonically modulated barrier at the origin, we have all ingredients needed in a generic stochastic-resonance model. Due to the above simplified implementation of the driving process, we are able to calculate the exact (nonlinear) response of the system. The response, which is the mean particle's position, is not only sensitive to the noise level, but it also displays resonancelike features with respect to the parameters of the unperturbed potential.

In many situations the unperturbed potential has no center of reflection symmetry. For example, in the studies of the noise-induced transport in Brownian ratchets [4], the symmetry breaking has been identified as a key cause for getting a directed probability current. In our second example, we consider two *reflecting* boundaries, symmetrically located with respect to the origin, and a linear potential in between. Obviously, in a time-independent potential, the mean coordinate relaxes to a definite temperature-dependent equilibrium value. However, it is not *a priori* clear what happens if we add the harmonically modulated barrier at the origin. In this model, we have disclosed a phenomenon, which does not seem to be covered in the existing literature; namely, the external driving with zero time average induces a *nonzero* time-averaged shift of the mean coordinate. The shift is oriented against the unperturbed potential slope. Differently speaking, a definite portion of the external-field energy is trapped within the system. Symmetric input is combined

*Email address: chvosta@kmf.troja.mff.cuni.cz
†Email address: peter.reineker@physik.uni-ulm.de

with the diffusion dynamics and produces an effective force which ''elevates'' the particle against the potential force.

The paper is organized as follows. In Sec. II, we introduce the Green function formulation of the problem and we derive basic equations. The basic frame is quite general, i.e., the calculation is valid for any unperturbed potential and for any form of the input signal. The reading will be useful for researchers wishing to apply the modulated-step device in their own settings. The focus here is on the Green function that represents a complete description of the diffusion process. Starting at Sec. III, we restricted the analysis just on the particle's mean position (the output signal). Here we have derived our most original results concerning the above two specific diffusion problems. We give formulas describing the output and its dependence on the input frequency and amplitude, on the temperature, and on the parameters of the unperturbed potential. The focus is on resonancelike aspects of the output amplitude and of the above driving-induced force.

II. GENERAL POTENTIAL WITH A TIME-DEPENDENT DISCONTINUITY

In the Brownian-motion-type notation, the Fokker-Planck equation for the Green function $G(x,y;t)$ reads

$$\frac{\partial}{\partial t}G(x,y;t)=-\frac{\partial}{\partial x}\left\{-D\frac{\partial}{\partial x}G(x,y;t)-\frac{1}{\Gamma}\left[\frac{\partial U(x;t)}{\partial x}\right]G(x,y;t)\right\}. \quad (1)$$

Here $U(x;t)$ is the potential, i.e., $F(x;t)=-(\partial/\partial x)U(x,t)$ is the corresponding force. The curly-bracketed expression represents the probability current $J(x,y;t)$. Γ equals the particle mass times the viscous friction coefficient. The thermal-noise strength parameter D increases linearly with the temperature, $D=k_BT/\Gamma$. The initial conditions are imposed at time $t_0=0$, i.e., we require $\lim_{t\to 0^+}G(x,y;t)=\delta(x-y)$. Boundary conditions will be discussed below.

A. Unperturbed problem and its solution

Let $U_1(x)$ and $U_2(x)$ be two arbitrary time-independent and space-continuous potentials. Without any loss of generality, assume that they coincide at $x=s$, i.e., $U_1(s)=U_2(s)$. As the first preparatory step, consider a combined space-continuous potential

$$U^{(0)}(x)=U_1(x)[1-\Theta(x-s)]+U_2(x)\Theta(x-s), \quad (2)$$

where $\Theta(x)$ is the right-continuous unit-step function: $\Theta(x)=1$ for $x\geqslant 0$ and $\Theta(x)=0$ for $x<0$. The analysis of the diffusion in this potential will be referred to as the *unperturbed* problem. Its solution consists in finding the Green function $G^{(0)}(x,y;t)$, which solves Eq. (1), and in calculating the corresponding probability current $J^{(0)}(x,y;t)$. The problem must be supplemented by some boundary conditions. Typically, one assumes a definite type of boundary conditions, e.g., reflecting or absorbing conditions, at two points $x_1<s$ and $x_2>s$.

The construction of the unperturbed Green function is a well-known procedure. However, in order to introduce an appropriate frame for our main problem, we now revise the calculation in the following four steps.

The basic ingredients are the Green functions $B_i(x,y;t)$ and the corresponding probability currents $C_i(x,y;t)$ for the two problems with the potentials $U_i(x)$, $i=1,2$. At x_1, the function $B_1(x,y;t)$ is required to fulfill the same boundary condition as that prescribed for the function $G^{(0)}(x,y;t)$. Moreover, one assumes that the natural boundary condition $\lim_{x\to+\infty}B_1(x,y;t)=0$. Similarly, $B_2(x,y;t)$ and $G^{(0)}(x,y;t)$ have to fulfill the same boundary condition at x_2, and moreover, one requires $\lim_{x\to-\infty}B_2(x,y;t)=0$. The first step consists in the calculation of the functions $B_i(x,y;t)$, and $C_i(x,y;t)$, $i=1,2$.

The second step starts by assuming an appropriate ansatz for the Laplace transforms $G^{(0)}(x,y;z)$ and $J^{(0)}(x,y;z)$. Here and below, we always use the notation $f(z)$ for the Laplace transformation of a time-dependent function $f(t)$; for clarity, the variables will be always quoted. The proper form of the ansatz depends on the relative positions of the points x, y, and s. For example, if $x\in(x_1;s)$ and $y\in(x_1;s)$, the assumed form will be designated as $G_{11}^{(0)}(x,y;z)$, if $x\in(x_1;s)$ and $y\in(s;x_2)$, we introduce $G_{12}^{(0)}(x,y;z)$, etc. Using this convention, the ansatz reads

$$G_{11}^{(0)}(x,y;z)=B_1(x,y;z)+B_1(x,s;z)Q_{11}^{(0)}(s,y;z), \quad (3)$$

$$G_{12}^{(0)}(x,y;z)=B_1(x,s;z)Q_{12}^{(0)}(s,y;z), \quad (4)$$

$$G_{21}^{(0)}(x,y;z)=B_2(x,s;z)Q_{21}^{(0)}(s,y;z), \quad (5)$$

$$G_{22}^{(0)}(x,y;z)=B_2(x,y;z)+B_2(x,s;z)Q_{22}^{(0)}(s,y;z). \quad (6)$$

Here $Q_{ij}^{(0)}(s,y;z)$ are the four functions to be specified below. Analogous relations express the assumed form of the probability current $J_{ij}^{(0)}(x,y;z)$; we simply replace $B_i(x,y;z)$ and $B_i(x,s;z)$ on the right-hand sides (RHS) by $C_i(x,y;z)$ and $C_i(x,s;z)$, respectively.

In the third step, one invokes the matching conditions $G^{(0)}(s-\epsilon,y;t)=G^{(0)}(s+\epsilon,y;t)$ and $J^{(0)}(s-\epsilon,y;t)=J^{(0)}(s+\epsilon,y;t)$, which guarantee the continuity of the probability density and of the probability current at the point $x=s$. Here ϵ is a positive infinitesimal parameter. In the following, we always implicitly assume the limit $\epsilon\to 0$ whenever the limit yields a well-defined analytical behavior of the resulting expression. Inserting the ansatz (3)–(6) into the matching conditions, one ends with the matrix equation

$$\begin{pmatrix}\beta_1(s;z) & -\beta_2(s;z)\\ \gamma_1(s;z) & -\gamma_2(s;z)\end{pmatrix}\begin{pmatrix}Q_{11}^{(0)}(s,y;z) & Q_{12}^{(0)}(s,y;z)\\ Q_{21}^{(0)}(s,y;z) & Q_{22}^{(0)}(s,y;z)\end{pmatrix}=\begin{pmatrix}-B_1(s,y;z) & B_2(s,y;z)\\ -C_1(s,y;z) & C_2(s,y;z)\end{pmatrix}. \quad (7)$$

Here we have introduced the abbreviations $\beta_1(s;z)=B_1(s-\epsilon,s;z)$, $\beta_2(s;z)=B_2(s+\epsilon,s;z)$, $\gamma_1(s;z)=C_1(s-\epsilon,s;z)$, and $\gamma_2(s;z)=C_2(s+\epsilon,s;z)$. These four functions shall be

called the *matching* functions. In fact, they describe the original diffusion processes [i.e., those with the potentials $U_i(x)$, $i=1,2$] in the vicinity of the point $x=s$. Note that their combination

$$\chi(s;z)=-\frac{\beta_1(s;z)\gamma_2(s;z)}{\beta_2(s;z)\gamma_1(s;z)}. \tag{8}$$

displays an extremely important property; namely, $\chi(s;z)=1$ if and only if the point $x=s$ represents the center of reflection for the unperturbed problem. Actually, in this case, one has $\beta_1(s;t)=\beta_2(s;t)$ and $\gamma_1(s;t)=-\gamma_2(s;t)$.

It is now a matter of simple algebra to solve the matrix equation (7) for $Q_{ij}^{(0)}(s,y;z)$. Performing this fourth step, one arrives at the final form of the Laplace-transformed unperturbed Green function:

$$G_{11}^{(0)}(x,y;z)=B_1(x,y;z)+\frac{B_1(x,s;z)}{1+\chi(s;z)}\left\{-\frac{\chi(s;z)}{\beta_1(s;z)}B_1(s,y;z)-\frac{1}{\gamma_1(s;z)}C_1(s,y;z)\right\}, \tag{9}$$

$$G_{12}^{(0)}(x,y;z)=\frac{B_1(x,s;z)}{1+\chi(s;z)}\left\{+\frac{\chi(s;z)}{\beta_1(s;z)}B_2(s,y;z)+\frac{1}{\gamma_1(s;z)}C_2(s,y;z)\right\}, \tag{10}$$

$$G_{21}^{(0)}(x,y;z)=\frac{B_2(x,s;z)}{1+\chi(s;z)}\left\{+\frac{1}{\beta_1(s;z)}B_1(s,y;z)+\frac{\chi(s;z)}{\gamma_2(s;z)}C_1(s,y;z)\right\}, \tag{11}$$

$$G_{22}^{(0)}(x,y;z)=B_2(x,y;z)+\frac{B_2(x,s;z)}{1+\chi(s;z)}\left\{-\frac{1}{\beta_2(s;z)}B_2(s,y;z)-\frac{\chi(s;z)}{\gamma_2(s;z)}C_2(s,y;z)\right\}. \tag{12}$$

B. Time-dependent discontinuity

We now supplement the unperturbed potential (2) with a time-dependent discontinuity at $x=s$. The height of the step will be controlled by a prescribed function, say $U_s(t)$. Altogether, we are faced with the diffusion problem in the time-dependent potential (the factor 2 on the RHS is introduced for later convenience)

$$U(x;t)=[U_1(x)+2U_s(t)][1-\Theta(x-s)]+U_2(x)\Theta(x-s). \tag{13}$$

We want to calculate the Green function $G(x,y;z)$ which solves Eq. (1) with potential (13).

The first two steps of this calculation are identical as before. We assume the form (3)–(6) with $G_{ij}(x,y;z)$ and $Q_{ij}(s,y;z)$, instead of $G_{ij}^{(0)}(x,y;z)$ and $Q_{ij}^{(0)}(s,y;z)$, respectively. The matching condition for the probability current is again $J(s-\epsilon,y;t)=J(s+\epsilon,y;t)$ and can be immediately Laplace transformed. However, as for the probability density, the jump condition [9] implies the relationship $G(s-\epsilon,y;t)=\xi(t)G(s+\epsilon,y;t)$, with $\xi(t)=\exp[-2U_s(t)/(k_BT)]$. Here comes the principal difficulty. The latter condition cannot be easily Laplace transformed and the subsequent analysis must be carried out in the time domain. Henceforth we express the jump conditions using the time-dependent form of the ansatz. This yields a matrix integral equation

$$\int_0^t\begin{pmatrix}\beta_1(s;t-t') & -\xi(t)\beta_2(s;t-t')\\ \gamma_1(s;t-t') & -\gamma_2(s;t-t')\end{pmatrix}\times\begin{pmatrix}Q_{11}(s,y;t') & Q_{12}(s,y;t')\\ Q_{21}(s,y;t') & Q_{22}(s,y;t')\end{pmatrix}dt'=\begin{pmatrix}-B_1(s,y;t) & \xi(t)B_2(s,y;t)\\ -C_1(s,y;t) & C_2(s,y;t)\end{pmatrix}. \tag{14}$$

Of course, it is always possible to write $\xi(t)=1-[1-\xi(t)]$ on the both sides of the equation and thus introduce a partitioning of the unknown functions $Q_{ij}(s,y;t)=Q_{ij}^{(0)}(s,y;t)+Q_{ij}^{(1)}(s,y;t)$. The perturbed part will be proportional to $[1-\xi(t)]$, i.e., it will vanish for the continuous potential. The unperturbed part is known from the preceding section. Hence it is possible to derive the integral equations for the perturbed matrix $Q^{(1)}(s,y;t)$ alone. Two of the four ensuing equations do not depend on $\xi(t)$. They can still be Laplace transformed and then used to eliminate two unknown functions. Namely, we have

$$Q_{21}^{(1)}(s,y;z)=\frac{\gamma_1(s;z)}{\gamma_2(s,z)}Q_{11}^{(1)}(s,y;z),$$

$$Q_{22}^{(1)}(s,y;z)=\frac{\gamma_1(s;z)}{\gamma_2(s,z)}Q_{12}^{(1)}(s,y;z). \tag{15}$$

After the elimination, the problem is reduced to the solution of just two Volterra integral equations of the second kind. Introducing the transformations

$$W_1(s,y;z)=-\beta_1(s;z)\frac{1+\chi(s;z)}{\chi(s;z)}Q_{11}^{(1)}(s,y;z),$$

$$W_2(s,y;z)=-\beta_1(s;z)\frac{1+\chi(s;z)}{\chi(s;z)}Q_{12}^{(1)}(s,y;z), \tag{16}$$

the integral equations assume a fairly compact final form

$$W_i(s,y;t)-\phi(t)\int_0^t\psi(s;t-t')W_i(s,y;t')dt'=\phi(t)R_i(s,y;t). \tag{17}$$

The kernel $K(t,t')=\phi(t)\psi(s;t-t')$ is a product of two functions. The first one $\phi(t)=\tanh[U_s(t)/(k_BT)]$ is the only function through which the time-dependent jump of the potential enters all the subsequent results. This function also modulates the RHS of the integral equation.

The Laplace transform of the second factor reads

$$\psi(s;z)=\frac{[1-\chi(s;z)]}{[1+\chi(s;z)]}=\frac{\beta_2(s;z)\gamma_1(s;z)+\beta_1(s;z)\gamma_2(s;z)}{\beta_2(s;z)\gamma_1(s;z)-\beta_1(s;z)\gamma_2(s;z)}. \tag{18}$$

This combination of the matching functions describes the asymmetry of the unperturbed problem. In problems with a center of reflection, one has $\chi(s;z)=1$, and hence $\psi(s;t)=0$. In these situations, the solution of the integral equation collapses to $W_i(s,y;t)=\phi(t)R_i(s,y;t)$.

On the RHS of the integral equation, Eq. (17), we have introduced the functions

$$R_1(s,y;z)=\frac{1}{1+\chi(s;z)}\left\{B_1(s,y;z)-\frac{\beta_1(s;z)}{\gamma_1(s;z)}C_1(s,y;z)\right\}, \tag{19}$$

$$R_2(s,y;z)=\frac{\chi(s;z)}{1+\chi(s;z)}\left\{B_2(s,y;z)-\frac{\beta_2(s;z)}{\gamma_2(s;z)}C_2(s,y;z)\right\}. \tag{20}$$

Finally, the transformations (16) have also invoked modifications of the functions $B_i(x,s;z)$ in the ansatz equations. The final result (see below) will be formulated by means of the two x-dependent functions

$$V_1(x,s;z)=-\frac{2\chi(s;z)}{1+\chi(s;z)}\frac{B_1(x,s;z)}{\beta_1(s;z)},$$

$$V_2(x,s;z)=\frac{2}{1+\chi(s;z)}\frac{B_2(x,s;z)}{\beta_2(s;z)}. \tag{21}$$

Let us now summarize the main results of the present Section. The target Green function has been partitioned as

$$G_{ij}(x,y;t)=G_{ij}^{(0)}(x,y;t)+\int_0^t dt' V_i(x,s;t-t')W_j(s,y;t'). \tag{22}$$

The unperturbed part describes the diffusion dynamics in the space-continuous time-independent potential (2). Its Laplace transformation is given by the formulas (9)–(12). The Laplace transformation of the perturbed part can be written as a product of two factors, i.e., $G_{ij}^{(1)}(x,y;z)=V_i(x,s;z)W_j(s,y;z)$. Here $W_i(s,y;t)$, $i=1,2$, are solutions of integral equation (17), and $V_j(x,s;z)$ are defined in Eqs. (21). The results are valid for any form of the unperturbed potential and for any time-dependent step-height function $U_s(t)$.

III. LINEAR POTENTIALS, REFLECTING BOUNDARIES, AND HARMONIC PERTURBATION

One of our motivations for the present study was an exact analysis of the nonlinear response with respect to the harmonically modulated input signal. In our setting, the input signal is the step-height function $U_s(t)$. Hence, starting from this point, we take it as $U_s(t)=K\cos(\omega t)$, with K being the amplitude and ω the angular frequency. Thereupon, the function $\phi(t)$ in the integral equation (17) assumes the form $\phi(t)=\tanh[\kappa\cos(\omega t)]$. Here the dimensionless parameter $\kappa=K/(k_BT)$ measures the temperature-reduced amplitude of the input signal and will be considered as the perturbation parameter. The function $\phi(t)$ can be expanded in powers of the parameter κ. However, it is also possible to write it as a sum of odd harmonics. Actually, we have

$$\begin{aligned}\phi(t)&=\sum_{k=1}^{\infty}\phi_k(\kappa)\cos(\omega_k t)\\&=\left[\kappa-\frac{\kappa^3}{16}+\frac{\kappa^5}{192}-\cdots\right]\cos(\omega t)\\&\quad+\left[-\frac{\kappa^3}{48}+\frac{\kappa^5}{384}-\cdots\right]\cos(3\omega t)+\cdots,\end{aligned} \tag{23}$$

with $\omega_k=(2k-1)\omega$. Note the κ expansion of the amplitudes $\phi_k(\kappa)$ starts with the term proportional to κ^{2k-1}.

In connection with the above mentioned focus of the present paper we now introduce three additional assumptions. First, the discontinuity will be placed at the origin, i.e., we set $s=0$. In order to make the following formulas more transparent, we skip quoting the dependence on s. Thus, e.g., $\chi(s;z)$ in Eq. (8) and $\psi(s;t)$ in Eq. (17) will be written as $\chi(z)$ and $\psi(t)$, respectively. Second, we shall introduce two reflecting boundaries at the coordinates $x_1=-l_1<0$ and $x_2=l_2>0$, i.e., the diffusion will be restricted to two neighboring domains of generally different widths, located to the left and to the right of the origin. Third, we take the potentials $U_i(x)$ in Eq. (2) to be *linear*, possibly with different slopes. This means that, while diffusing within the left (right) region, the particle is acted upon with a *constant* force F_1 (F_2). For example, if $l_i\to\infty$, $i=1,2$, and $F_1=-F_2>0$, the unperturbed problem represents the diffusion in a V-shaped continuous potential with the tip located at the origin.

At this point, a brief comment is needed concerning our third assumption. The idea of using the piecewise linear potential to study noise-induced phenomena has been exploited by several authors. Diffusion dynamics in the time-independent piecewise linear potential has been studied, e.g., in [10–12]. Using the Laplace-transform method, these problems, including various types of boundaries, are analytically tractable. The calculation is more involved, if the slope of the linear potential depends on time. The additional influence can be either *coherent* (e.g., an external sinusoidal driving) or *stochastic* (e.g., an intrinsic random modulation of the potential profile). In the first case, one possible approach operates with the powerful Floquet theory together with the eigenfunction treatment of the unperturbed problem [13]. Another possibility would be an approximation of the sinusoidal signal by a piecewise constant periodic function [14]. Anyway, typically, the coherent-driving models with linear potentials are not analytically solvable. As for the stochastic modulation of the linear-potential slope, the setting is often assumed in the analysis of the resonant-activation phenomenon [15–19]. In these problems, again, the Laplace-transform method usually leads to exact results. The strategy we shall adopt in the remainder of this paper is as follows.

The generic features of the problems with coherently modulated slopes of the linear potentials are preserved if the slopes are fixed and, instead, if one modulates the discontinuity connecting the different slopes. The idea of the time-modulated discontinuity has been used in Refs. [20] and [21]. However, these authors operate with piecewise constant potentials (zero slope) and they invoke a perturbationlike treatment of the step-modulation amplitude.

Let us now incorporate these assumptions into the equations of the preceding section. We need two Green functions $B_i(x,y;t)$, and two probability currents $C_i(x,y;t)$, $i=1,2$ for the two linear potentials $U_i(x)=-F_i x$. As for the potential $U_1(x)$, we assume the reflecting boundary at $x_1=-l_1$ and the natural boundary at plus infinity. Similarly, for the diffusion in the potential $U_2(x)$, we place the reflection boundary at $x_2=l_2$ and the natural boundary at minus infinity. The following formulas display the Laplace transformations of the needed functions.

$$B_1(x,y;z)=D_1(x,y;z)+\frac{1}{2D\alpha_1(z)}\frac{\alpha_1^-(z)}{\alpha_1^+(z)}\times\lambda_1(z)e^{-x\alpha_1^-(z)}e^{-y\alpha_1^+(z)}, \tag{24}$$

$$B_2(x,y;z)=D_2(x,y;z)+\frac{1}{2D\alpha_2(z)}\frac{\alpha_2^+(z)}{\alpha_2^-(z)}\times\lambda_2(z)e^{x\alpha_2^+(z)}e^{y\alpha_2^-(z)}, \tag{25}$$

$$C_1(x,y;z)=E_1(x,y;z)+\frac{1}{2\alpha_1(z)}\times\alpha_1^-(z)\lambda_1(z)e^{-x\alpha_1^-(z)}e^{-y\alpha_1^+(z)}, \tag{26}$$

$$C_2(x,y;z)=E_2(x,y;z)-\frac{1}{2\alpha_2(z)}\alpha_2^+(z)\lambda_2(z)e^{x\alpha_2^+(z)}e^{y\alpha_2^-(z)}. \tag{27}$$

Here $\alpha_i(z)=\sqrt{z/D+a_i^2}$, $a_i=F_i/(2D\Gamma)$, $\alpha_i^{\pm}(z)=\alpha_i(z)\pm a_i$, and $\lambda_i(z)=\exp[-2l_i\alpha_i(z)]$. The Green functions $D_i(x,y;z)$, $i=1,2$ and the probability currents $E_i(x,y;z)$ are solutions of two problems with linear potentials $U_i(x)=-F_i x$ and with natural boundary conditions $\lim_{x\to\pm\infty}D_i(x,y;t)=0$. Thus, $D_i(x,y;t)$ simply describes the spreading probability-density packet whose center drifts with constant velocity F_i/Γ. By Laplace transforming the corresponding Fokker-Planck equations and then solving the emerging ordinary differential equation one easily obtains

$$D_i(x,y;z)=\frac{1}{2D\alpha_i(z)}\{\Theta(y-x)e^{-(y-x)\alpha_i^+(z)}+\Theta(x-y)e^{-(x-y)\alpha_i^-(z)}\}, \tag{28}$$

$$E_i(x,y;z)=\frac{1}{2\alpha_i(z)}\{-\Theta(y-x)\alpha_i^-(z)e^{-(y-x)\alpha_i^+(z)}+\Theta(x-y)\alpha_i^+(z)e^{-(x-y)\alpha_i^-(z)}\}. \tag{29}$$

Moreover, we shall need the four matching functions which appear above Eq. 8. Their present forms read

$$\beta_1(z)=\frac{1}{2D\alpha_1(z)}\left[1+\frac{\alpha_1^-(z)}{\alpha_1^+(z)}\lambda_1(z)\right], \tag{30}$$

$$\beta_2(z)=\frac{1}{2D\alpha_2(z)}\left[1+\frac{\alpha_2^+(z)}{\alpha_2^-(z)}\lambda_2(z)\right], \tag{31}$$

$$\gamma_1(z)=-\frac{\alpha_1^-(z)}{2\alpha_1(z)}[1-\lambda_1(z)], \tag{32}$$

$$\gamma_2(z)=\frac{\alpha_2^+(z)}{2\alpha_2(z)}[1-\lambda_2(z)], \tag{33}$$

and therefore their combination (8) is

$$\chi(z)=\frac{[\alpha_1^+(z)+\alpha_1^-(z)\lambda_1(z)][1-\lambda_2(z)]}{[\alpha_2^-(z)+\alpha_2^+(z)\lambda_2(z)][1-\lambda_1(z)]}. \tag{34}$$

Note that this function actually equals unity if and only if the two regions have the same width, i.e., $l_1=l_2$, and the slopes of the linear potentials within these regions are opposite, i.e., $F_1=-F_2$.

The functions (23)–(34) yield everything that is needed in the integral equation (17). We assume, for the moment, that the integral equation has been solved, i.e., we know the resulting Green function $G(x,y;t)$. Then we have the complete information about the diffusion process. For example, one can inquire, what portions of the total probability mass are, at a given time, situated on the right (on the left) from the origin. However, remembering again our main objective, we shall concentrate on the calculation of the particle's mean position $\mu(y;t)=\int_{-l_1}^{l_2}dx\,x\,G(x,y;t)$. This function will be referred to as the *output signal*. Using the partitioning (22), the output signal splits as $\mu(y;t)=\mu^{(0)}(y;t)+\mu^{(1)}(y;t)$. The unperturbed part relaxes to a given value which is dictated by Gibb's equilibrium distribution; namely, this temperature-dependent value is

$$\mu_s^{(0)}=\lim_{t\to\infty}\mu^{(0)}(y;t)=\frac{\int_{-l_1}^{l_2}dx\,x\exp[-U^{(0)}(x)/(k_BT)]}{\int_{-l_1}^{l_2}dx\exp[-U^{(0)}(x)/(k_BT)]}. \tag{35}$$

The potential $U^{(0)}(x)$ is piecewise linear and hence the equilibrium mean position can be easily evaluated.

As for the perturbed part, the results from the preceding section lead to the expression

$$\mu^{(1)}(y;t)=\int_0^t dt'\left[\int_{-l_1}^0 dx\, xV_1(x;t-t')+\int_0^{l_2} dx\, xV_2(x;t-t')\right]W_i(y;t')$$
$$=\int_0^t dt' M(t-t')W_i(y;t'), \tag{36}$$

with $V_i(x;z)$ being given in Eqs. (21). The result of the x-integration reads

$$M(z)=\frac{2D}{z}\frac{\dfrac{\alpha_1^-(z)+\alpha_1^+(z)\lambda_1(z)-2\alpha_1(z)e^{-l_1\alpha_1^+(z)}}{1-\lambda_1(z)}+\dfrac{\alpha_2^+(z)+\alpha_2^-(z)\lambda_2(z)-2\alpha_2(z)e^{-l_2\alpha_2^-(z)}}{1-\lambda_2(z)}}{\dfrac{\alpha_1^+(z)+\alpha_1^-(z)\lambda_1(z)}{1-\lambda_1(z)}+\dfrac{\alpha_2^-(z)+\alpha_2^+(z)\lambda_2(z)}{1-\lambda_2(z)}}. \tag{37}$$

We have quoted this complex expression because all the subsequent results rest on the asymptotic analysis of the last two formulas. Typically, the perturbed part of the output displays transitory effects superimposed with the stationary part, i.e., $\mu^{(1)}(y;t)=\mu^{(1)}_{trans}(y;t)+\mu^{(1)}_s(t)$. In the time-asymptotic region, the transitory part vanishes and the whole output assumes its stationary form $\mu_s(t)=\mu_s^{(0)}+\mu_s^{(1)}(t)$. The stationary output will be shown to display quite remarkable features.

A. Stochastic resonance

Assume $l_1=l_2=l$ and $F_1=-F_2=F$. The unperturbed potential forms a symmetric tip at the origin. The tip points down (up) for F positive (negative), i.e., we can speak about V potential (Λ potential) with the minimum (maximum) at the origin. Let us concentrate, for the moment, on the up-directed tip (all the calculation below is valid for an arbitrary sign of the force). Then the linear potentials at both sides of the origin together with the reflecting barriers mimic a double-well symmetric potential. Adding the time-dependent discontinuity at the origin, we are faced with an archetypical stochastic-resonance setting [7]. During each half period when the step-height function $U_s(t)$ is positive (negative), the discontinuity acts as a potential barrier for the diffusion trajectories approaching it from the right (from the left). In our setting, the height of the barrier will harmonically oscillate and Fig. 1 illustrates the space and the time dependence of the whole potential.

As mentioned above, in the present setting, the origin represents a center of reflection for the unperturbed problem. Consequently, the unperturbed equilibrium probability density is an even function and the equilibrium mean position $\mu_s^{(0)}$ in Eq. (35) vanishes. Second, the function $\chi(z)$ in Eq. (17) vanishes also and Eqs. (36) simply read

$$\mu^{(1)}(y;t)=\int_0^t dt' M(t-t')\phi(t')R(y;t')$$
$$=\sum_{k=1}^{\infty}\phi_k(\kappa)\int_0^t dt' M(t-t')\cos(\omega_k t')R(y;t'). \tag{38}$$

Here we have already inserted the expansion (23).

In order to simplify the notation, we introduce $\alpha(z)=\sqrt{z/D+a^2}$, with $a=F/(2D\Gamma)$, $\alpha^{\pm}(z)=\alpha(z)\pm a$, and $\lambda(z)=\exp[-2l\alpha(z)]$. Hence, comparing with the text below Eq. (27), we have $\alpha_1^{\pm}(z)=\alpha^{\pm}(z)$, $\alpha_2^{\pm}(z)=\alpha^{\mp}(z)$, and $\lambda_1(z)=\lambda_2(z)=\lambda(z)$. Using all this in Eq. (37), we get

$$M(z)=\frac{2D}{z}\frac{\alpha^-(z)+\lambda(z)\alpha^+(z)-2\alpha(z)e^{-l\alpha^+(z)}}{\alpha^+(z)+\lambda(z)\alpha^-(z)}. \tag{39}$$

Performing a detailed analysis, one can prove that there is no pole of this function at the origin of the complex plane. Finally, in the present case, the functions (19) and (20) are identical, i.e., $R_1(y;z)=R_2(y;z)$, their common form being

$$R(y;z)=\frac{1}{2z}\frac{\alpha^+(z)e^{-|y|\alpha^-(z)}+\alpha^-(z)\lambda(z)e^{|y|\alpha^+(z)}}{1-\lambda(z)}. \tag{40}$$

This function displays the first-order pole at the origin.

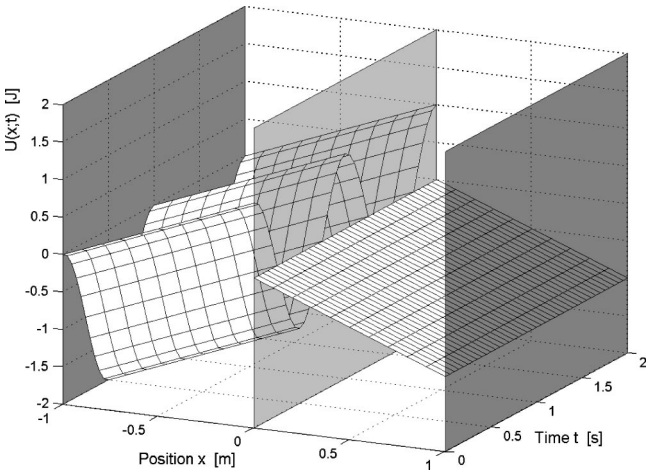

FIG. 1. The time-modulated potential $U(x;t)$ as considered in this section. We took $l=1\,\mathrm{m}$, $F=-1\,\mathrm{N}$, $\omega=2\pi\ \mathrm{rad\,s^{-1}}$, and $K=0.5\,\mathrm{J}$. The two darker planes at $x=\pm l$ are the two reflecting walls. The central plane at $x=0\,\mathrm{m}$ is included for clarity.

We now turn to the calculation of the convolution integral in Eq. (38). Upon writing $\cos(\omega_k t)$ as a sum of two exponentials, the formula (38) can be Laplace transformed and we arrive at the problem of the asymptotic behavior of a function which is known to have first-orders poles at $z=\pm i\omega_k$ due to the terms $R(y;z\pm i\omega_k)$. Introducing an appropriate contour in the complex plane and applying the residuum theorem [22], one can separate the transitory part of the results (this emerges from the integrals along both sides of the negative imaginary axis) and the oscillatory part (stemming from the residua at the poles). The latter part already represents the stationary output signal. Skipping all details, the final result of the present section reads

$$\mu_s(t)=\sum_{k=1}^{\infty} A_k(\omega)\cos[\omega_k t-\Psi_k(\omega)]. \tag{41}$$

In words, the time-asymptotic output signal contains the fundamental frequency and its odd harmonics. The amplitude $A_k(\omega)$ is proportional to the perturbation factor $\phi_k(\kappa)$. Apart from this dependence, the amplitudes and the phase shifts are controlled by just two generic functions which are evaluated at the equidistant points ω_k. More precisely, we have

$$A_k(\omega)=\phi_k(\kappa)\frac{a}{1-e^{-2la}}|M(i\omega_k)|,$$

$$\sin\Psi_k(\omega)=-\frac{\mathrm{Im}[M(i\omega_k)]}{|M(i\omega_k)|},\quad \cos\Psi_k(\omega)=\frac{\mathrm{Re}[M(i\omega_k)]}{|M(i\omega_k)|}, \tag{42}$$

$\mathrm{Re}[M(z)]$ and $\mathrm{Im}[M(z)]$ being the real and the imaginary part of the function (39), respectively. The combination $2l|a|=l|F|/(k_BT)$ represents the (negative) temperature-reduced height of the potential tip for the unperturbed problem.

Remembering that the κ expansion of the function $\phi_k(\kappa)$ begins with the power κ^{2k-1}, Eqs. (41) and (42) contain the *linear*-response output. Actually, in the linear response, the terms with $k>1$ in Eq. (41) are not considered and, in the first term, we take $\phi_1(\kappa)\approx\kappa$. Thus the linear response is simply given by phase-shifted oscillations with the fundamental frequency. We now write the linear-response amplitude in a form which will be well suited for a further analysis. The form reads

$$\begin{aligned}A^{(lr)}(\omega)&=\frac{4K}{|F|}\left\{\frac{\Xi^2}{\exp(\Xi)-1}\right\}\\&\quad\times\left\{\frac{1}{\Theta}\left|\frac{\tilde\alpha^-+\tilde\lambda\tilde\alpha^+-2\tilde\alpha\exp(-\tilde\alpha^+/2)}{\tilde\alpha^++\tilde\lambda\tilde\alpha^-}\right|\right\}\\&=\frac{4K}{|F|}\mathcal{A}_1(\Xi)\mathcal{A}_2(\Xi,\Theta).\end{aligned} \tag{43}$$

Here $\tilde\alpha=\sqrt{\Xi^2+i\Theta}$, $\tilde\alpha^{\pm}=\tilde\alpha\pm\mathrm{sgn}(F)\Xi$, and $\tilde\lambda=\exp(-\tilde\alpha)$. We have introduced two important dimensionless parameters. First, $\Xi=2l|a|=l|F|/(k_BT)$ represents the temperature-reduced height of the potential barrier (for $F<0$) or the temperature-reduced depth of the potential well (for $F>0$). In the former case, the parameter Ξ controls the Kramers time τ_K for surmounting the unperturbed potential barrier. More precisely, the Kramers time is proportional to $\exp(\Xi)$ [10]. Second, the parameter $\Theta=4l^2\omega/D$ reflects the ratio between the time scale for the potential modulation, $\tau_\omega\propto 1/\omega$, and the time scale $\tau_D\propto l^2/D$ for the diffusive spreading within the spatial domain $(-l;l)$. For example, if $\Theta\gg 1$, the external modulation is rapid with respect to the diffusion, if $\Theta\ll 1$, the driving is slow (the adiabatic limit). Equation (43) describes a nontrivial competition between all the three time scales. Further discussion will be given below.

To illustrate our results, in Fig. 2, we shall first focus on the particle's mean position and present several typical features. The data were obtained by the numerical Laplace inversion of the functions $R(y;z)$, Eq. (40), and $M(z)$, Eq. (39), followed by the numerical evaluation of the convolution integral in Eq. (38).

As follows from the preceding calculation, if $\kappa\gg 1$, the output displays highly nonlinear features. In the strong driving regime, the coefficients $\phi_k(\omega)$ are not negligible and thus the output contains higher harmonics. This can be also seen in the spectral analysis of the output. Let us briefly discuss the four panels in Fig. 2.

Panel (a) demonstrates a typical form of the transitory effects. Of course, they are not present in the linear-response curve, as this curve is already calculated in the asymptotic-time limit. Panel (b) compares two curves evaluated for the two different temperatures. The remaining parameters were tuned in such way, that the comparison shows up the stochastic resonance effect; namely, by *increasing* the temperature, there occurs a synchronization between the temperature-induced interwell transitions and the input signal. As a result, the amplitude of the periodic output *increases*. No such increase can occur in the *V*-potential model. Panel (c) demonstrates that the increase of the output amplitude can also occur by increasing the unperturbed barrier height. For F negative, this is not surprising as the increase of the potential barrier $|F|l$ is effectively equivalent with a decrease of the temperature. Panel (d) displays typical differences between the diffusion *V*-shaped and Λ-shaped unperturbed potential. In the first case, there is no potential barrier and hence the instantaneous, e.g., positive, value of the input $U_s(t)=K\cos(\omega t)$ leads to an immediate motion of the probability mass to the right. Contrary to this, having a potential barrier in the unperturbed Λ potential, the stationary output displays a significant phase delay with respect to the input.

Let us now return to the discussion of resonances. Our analysis will be based on Eq. (43) and we consider, first, the case $F<0$ (i.e., the Λ-shaped unperturbed potential). On the RHS we recognize a product of two functions. The first one, $\mathcal{A}_1(\Xi)=\Xi^2/(\exp(\Xi)-1)$, displays maximum at the point $\Xi^\star$ which solves the equation $1-\exp(-\Xi)=\Xi/2$, i.e., $\Xi^\star\in(1,2)$. If we treat $\mathcal{A}_1(\Xi)$ as a function of the noise inten-

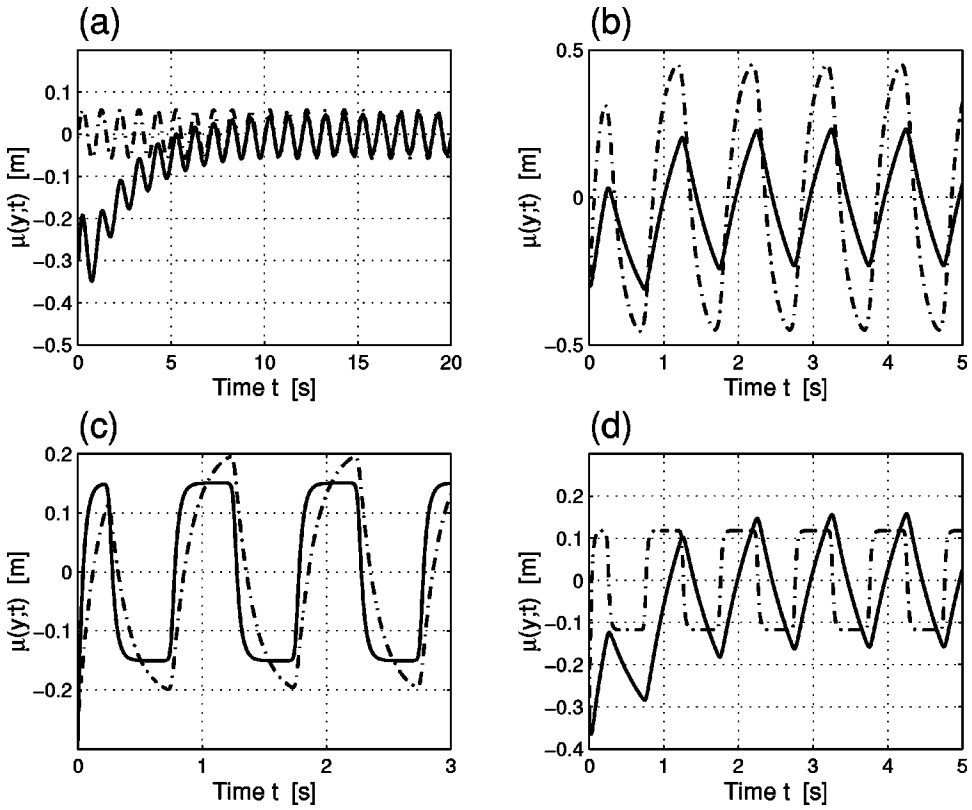

FIG. 2. Time dependence of the particle's mean position. In all panels, the input frequency is $\omega=2\pi$ rad s^{-1}, $\Gamma=1$ kg s^{-1}, and the initial position is $y=-0.3$ m. Panel (a) compares the exact solution (full curve) with the corresponding linear-response result (broken curve). For both the curves, the parameters are $D=1.0$ m^2 s^{-1}, $F=-0.5$ N, $l=2.0$ m, and $K=1.0$ J. Panel (b) demonstrates the increase of the output amplitude with increasing temperature. The full line has $D=1.0$ m^2 s^{-1}, and the broken one $D=3.0$ m^2 s^{-1}. Otherwise, we took $F=-0.5$ N, $l=1.0$ m, and $K=10.0$ J. Panel (c) exemplifies the increase of the output amplitude with increasing the unperturbed barrier height. Here we set $F=-0.05$ N (full curve) and $F=-10.0$ N (broken curve). Otherwise, we use $D=1.0$ m^2 s^{-1}, $l=0.3$ m, and $K=10.0$ J. Panel (d) illustrates typical differences between the dynamics in the monostable and in the bistable model. The full curve corresponds to Λ-shaped potential with $F=-5.0$ N, and the broken one to V-shaped potential with $F=10.0$ N. Both curves have $D=1.0$ m^2 s^{-1}, $l=0.6$ m, and $K=10.0$ J.

sity, the maximum occurs at $D^\star$, where $D^\star \in (l|F|/(2\Gamma), l|F|/\Gamma)$. The value $D^\star$ does not depend on the frequency of the potential modulation. However, due to the second factor in Eq. (43), the position of the maximum of the product $\mathcal{A}_1(\Xi)\mathcal{A}_2(\Xi,\Theta)$ is shifted with respect to the above value, $D^\star$. Actually, the second factor $\mathcal{A}_2(\Xi,\Theta)$ is a complicated function of the two variables indicated (they both are inversely proportional to D), but it displays finite nonzero limits

$$\lim_{D\to\infty}\mathcal{A}_2(\Xi,\Theta)=\frac{1}{8},\quad \lim_{D\to 0}\mathcal{A}_2(\Xi,\Theta)=\frac{F^2}{2l^2\omega^2\Gamma^2}\left|\sin\left(\frac{l\omega\Gamma}{2|F|}\right)\right|. \tag{44}$$

On the whole, the linear response amplitude (43) displays maximum at some point, say at $D_{sr}(\omega)$. Heuristically, if $\omega<0.5$ ($\omega>0.5$), the true maximum $D_{sr}(\omega)$ is shifted with respect to $D^\star$ towards lower (higher) values of the noise intensity. There is no simple analytical relation which would describe this frequency dependence. Qualitatively, the higher the frequency (the lower the period of the driving signal), the higher $D_{sr}(\omega)$, i.e., also the lower Kramers time τ_K. We thus recover the basic condition for the D-stochastic resonance [7]: the statistical synchronization occurs when the average waiting time between two noise-induced interwell transitions is comparable to the period of the driving signal.

Figure 3 shows the linear-response amplitude as a function of the temperature and the slope of the unperturbed potential. A similar peak has also been detected if the amplitude is displayed as a function of the width l. Generally speaking, besides on the frequency, the output amplitude depends on all further parameters, i.e., on K, F, $D\Gamma=k_BT$, and l. At the same time, due to the rather complicated structure of Eq. (43), the analytic expressions for the maxima would not be very illustrative.

The resonance in D occurs only if $F<0$. Contrary to this, keeping the temperature and the other parameters constant, the resonance in F can occur also for a positive F. The physical essence behind this effect is as follows. We assume first a sharp slope of the V-shaped unperturbed potential. Due to the large ''attractive'' force, the particle cannot migrate far from the origin and the amplitude of its mean-position oscillations

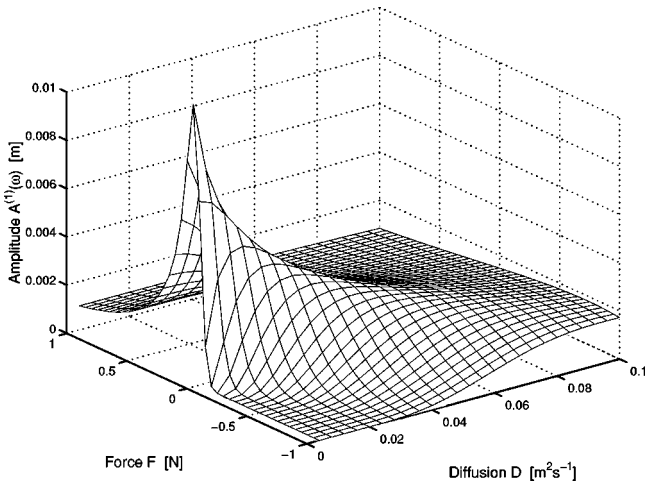

FIG. 3. The linear-response amplitude as a function of the diffusion constant D and the potential slope F. In the calculation, we took the amplitude of the step-height function $K=0.001$ J, the frequency of the time-dependent potential contribution $\omega=0.5$ rad s^{-1}, and the half-width of the whole diffusion region $l=0.3$ m. For a positive F, i.e., for the V-shaped unperturbed potential, there is no resonance with respect to the variable D.

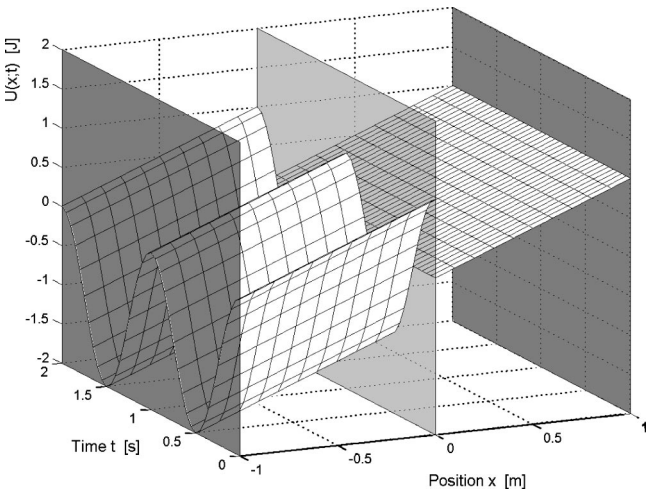

FIG. 4. The time-modulated potential $U(x;t)$ as considered in this section. We took $l=1$ m, $F=-1$ N, $\omega=2\pi$ rad s^{-1}, and $K=0.5$ J. The two darker planes at $x=\pm l$ are the two reflecting walls. The central plane at $x=0$ m is included for clarity.

is small. Second, we assume a flat minimum of the unperturbed potential. Then the particle performs relatively large excursions from the origin. However, the excursions occur *symmetrically* to both sides from the origin and hence they do not contribute to the mean position. Only a small portion of the probability density in the vicinity of the origin is nonsymmetrically affected by the oscillating barrier. On the whole, the amplitude of the particle's mean position is again small. In conclusion, there must exist an ''optimal'' slope for which the amplitude assumes its maximal value. This reasoning will only be valid if the width of the diffusion domain is sufficiently large.

The resonance peak in the variable l has a similar origin. We assume a negative F and a small l. Then, because of purely geometrical reasons, the output amplitude must be small. In the opposite case, i.e., assuming a sufficiently broad diffusion region $|a|l\gg 1$, a significant part of the probability mass is *symmetrically* distributed in domains that are far from the origin (i.e., close to the reflection boundaries). Only a small portion of the probability density in the vicinity of the origin is nonsymmetrically affected by the oscillating barrier. The corresponding contribution to the integral defining the mean position is also small. In conclusion, there must be an optimal width for which the amplitude assumes its maximal value. For positive F this reasoning goes to certain critical value of the collecting force. Above this value, no resonance in l occurs.

All these heuristic conclusions were confirmed by the explicit evaluation of the output amplitude (43).

B. Driving-induced force

In this section, we take again $l_1=l_2=l$, but now let $F_1=F_2=F$. Figure 4 illustrates the space and the time dependence of the potential in this case.

Therefore the potential for the unperturbed problem is simply a straight line in the symmetric diffusion domain of total width $2l$. If $F<0$ $(F>0)$, the force pushes the particle against the left (right) boundary. The equilibrium mean position for the unperturbed problem is given below, c.f., the first term on the RHS of Eq. (50). It is an odd function of the force, and it has the same sign as F. What happens if we add the oscillating discontinuity at the origin? One feels that the stationary response should again display some (nonlinear) oscillations. However, around *what* value? This is the central question of the present section.

Provided $F\neq 0$, the unperturbed problem has no center of reflection symmetry, the combination (34) is no longer zero, and we are faced with the integral equation (17) in their full form. We start again by calculating the present form of the function (37). Introducing $\alpha(z)=\sqrt{z/D+a^2}$, with $a=F/(2D\Gamma)$, $\alpha^{\pm}(z)=\alpha(z)\pm a$, and $\lambda(z)=\exp[-2l\alpha(z)]$, we have $\alpha_1(z)=\alpha_2(z)=\alpha(z)$, $\alpha_1^{\pm}(z)=\alpha_2^{\pm}(z)=\alpha^{\pm}(z)$, and $\lambda_1(z)=\lambda_2(z)=\lambda(z)$. Using all this in Eq. (37), we arrive at a quite transparent expression

$$M(z)=\frac{2D}{z}\left[1-\frac{\cosh(la)}{\cosh[l\alpha(z)]}\right]. \tag{45}$$

A detailed analysis shows that there is no pole of this function at the origin. Next, focusing on the integral equation (17), on the RHS we have

$$R_i(y;z)=\frac{1}{2z}\,\frac{\alpha^{\mp}(z)+\lambda(z)\alpha^{\pm}(z)}{\alpha(z)[1-\lambda^2(z)]}\left[\alpha^{\pm}(z)e^{-|y|\alpha^{\mp}(z)}+\alpha^{\mp}(z)\lambda(z)e^{|y|\alpha^{\pm}(z)}\right], \tag{46}$$

where the upper (the lower) sign is valid for $i=1$, i.e.,

$y<0$ (for $i=2$, i.e., $y\geqslant 0$). Finally, the expression (18) in the kernel of the integral equation (17) reads [22]

$$\psi(z)=-\frac{a}{\alpha(z)}\tanh[l\alpha(z)]\Rightarrow\psi(t)$$

$$=-\mathrm{sgn}(a)Da^2\frac{e^{-Da^2t}}{\sqrt{\pi Da^2t}}$$

$$\times\left[1+2\sum_{n=1}^{\infty}(-1)^n\exp\left(-n^2\frac{l^2}{Dt}\right)\right]. \qquad (47)$$

The kernel displays at $t=0$ a weak singularity of the form $\psi(t)\propto 1/\sqrt{\pi Dt}$.

We now start with the iterative solution of the integral equation (17). Formally, let the kernel be proportional to a parameter, say ζ. Then the Neumann series for the solution is $\Sigma_{k=0}^{\infty}W_{i,(k)}(y;t)$, where $W_{i,(k)}(y;t)\propto\zeta^k$. The zero-order term is simply given by the right of the integral equation, i.e., $W_{i,(0)}(y;t)=\phi(t)R_i(y;t)$. Inserting this term in Eq. (36) and using the same steps as in the preceding section, we get again a sum of odd harmonics, their amplitudes being proportional to $\phi_k(\kappa)$. At the same time, this is the only term which contributes to the linear-response output [the explicit form of the linear-response output is given in Eq. (52) below].

Next, let us consider the first iteration of the integral equation. We integrate the kernel $K(t,t')$ multiplied by the zero-order result $W_{i,(0)}(y;t)$. Inserting the mode expansion of the function $\phi(t)$, we have to calculate

$$W_{i,(1)}(y;t)=\sum_{m=1}^{\infty}\sum_{n=1}^{\infty}\phi_m(\kappa)\phi_n(\kappa)\cos(\omega_m t)$$

$$\times\int_0^t dt'\,\psi(t-t')\cos(\omega_n t')R_i(y;t'). \qquad (48)$$

Here comes the crucial point. We write again the function $\cos(\omega_m t)$ and $\cos(\omega_n t')$ as sums of two exponentials, and we carry out the Laplace transformation. The terms with $m\neq n$ have poles at $z=\mathrm{i}\omega_m\pm\mathrm{i}\omega_n$. Asymptotically, they contribute to the oscillatory part of the output. However, one part of the diagonal $m=n$ terms leads to the compensation of the two pole shifts in the expression $R_i(y;z\pm\mathrm{i}\omega_m\pm\mathrm{i}\omega_n)$. As a result, these terms will have pole at the origin of the complex plane. Inserting these terms into the convolution in Eq. (36) and using the residuum theorem, we end with an asymptotically surviving, nonoscillatory term

$$s_{(1)}(\omega)=\frac{l}{2\cosh^2(la)}\sum_{m=1}^{\infty}\phi_m^2(\kappa)\mathrm{Re}[\psi(\mathrm{i}\omega_m)]. \qquad (49)$$

The lower index reminds that we are discussing the contribution which is linear in the parameter ζ. However, at the same time, the expression is even in the perturbation parameter κ. Its κ expansion starts with the *quadratic* contribution.

In a similar way, we can analyze the higher-order iterations of the integral equation. Without going into details, let us now collect all the findings into one final formula. In the present symmetry-broken setting, the stationary output signal reads

$$\mu_s(t)=l\left[\coth(2la)-\frac{1}{2la}\right]+\sum_{k=1}^{\infty}s^{(2k)}(\omega)$$

$$+\sum_{k=1}^{\infty}S_k(\omega)\cos[k\omega t-\Phi_k(\omega)]. \qquad (50)$$

The first term is the equilibrium mean position $\mu_s^{(0)}$ of the unperturbed problem—it has been obtained by evaluating the integrals in Eq. (35). The second term is the κ expansion of the driving-induced shift $s(\omega)$, i.e., $s^{(2k)}(\omega)\propto\kappa^{2k}$ (note the distinct designation for the iteration expansion of the shift and the κ expansion). The lowest order (in κ) reads

$$s^{(2)}(\omega)=-l\kappa^2\frac{1}{2\cosh^2(la)}\frac{\rho_+(\omega)\sinh[2la\rho_+(\omega)]+\rho_-(\omega)\sin[2la\rho_-(\omega)]}{[\rho_+^2(\omega)+\rho_-^2(\omega)]\{\cosh[2la\rho^+(\omega)]+\cos[2la\rho^-(\omega)]\}}. \qquad (51)$$

Here we have used the abbreviations $\rho_\pm(\omega)=[(\Omega^2+1)^{1/2}\pm 1]^{1/2}/\sqrt{2}$, and $\Omega=\omega/(Da^2)$ is the temperature-reduced frequency. Finally, the oscillatory part in Eq. (50) includes both odd and even harmonics. The amplitudes of even (odd) harmonics are even (odd) functions of the parameter κ. The linear-response part of the last term contributes to the linear response. Quite explicitly, the linear-response of the system is

$$\mu_s^{(lr)}(t)=l\left[\coth(2la)-\frac{1}{2la}\right]$$

$$+\frac{a\kappa}{\sinh(2al)}|M(\mathrm{i}\omega)|\cos[\omega t-\Phi(\omega)]. \qquad (52)$$

The phase delay of the output behind the input is determined by the relations $\sin\Phi(\omega)=-\mathrm{Im}[M(\mathrm{i}\omega)]/|M(\mathrm{i}\omega)|$ and

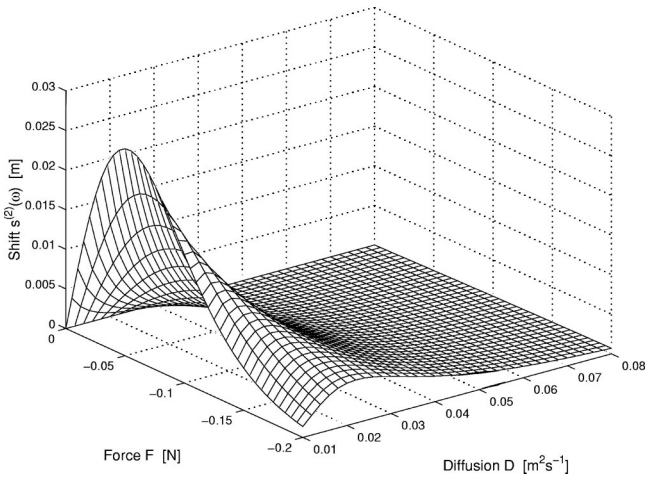

FIG. 5. The driving-induced shift $s^{(2)}$ as a function of the noise intensity D and the potential slope F. The calculation is based on Eq. (51). We took the amplitude of the step-height function $K=0.01$ J, the frequency of the step-height modulation $\omega=0.5$ rad s^{-1}, and the half-width of the whole diffusion region $l=0.3$ m.

$\cos\Phi(\omega)=\mathrm{Re}[M(i\omega)]/|M(i\omega)|$. Here $\mathrm{Re}[M(z)]$ and $\mathrm{Im}[M(z)]$ are the real and imaginary parts of the function (45), respectively.

Summing up, the exact stationary output exhibits periodic oscillations around the value $\mu_s^{(0)}+s(\omega)$. The driving-induced shift is always opposite to the force F; it is an odd function of the force, and an even function of the perturbation parameter κ. Figure 5 demonstrates its variations with changing temperature and/or the unperturbed slope of the potential. We have chosen special values of the parameters so that the shift shows off resonancelike features. The peak is caused by the synchronization of the driving and the time scales which control the unperturbed dynamics. The latter time scales are controlled not only by temperature but also by the force F and by the width of the diffusion region $2l$.

Let us perform the time average of the stationary output. Then all the terms which oscillate around zero will be removed. What remains is the sum of the unperturbed equilibrium value $\mu_s^{(0)}$ and the driving-induced shift $s(\omega)$. We can ask the following question. What time-independent force, say F_s, should be added to the original force F to induce the new equilibrium position $\mu_s^{(0)}+s(\omega)$? This force has purely dynamical origin. It can be explicitly calculated by solving the equation

$$\coth\left(\frac{lF}{\Gamma D}\right)-\coth\left[\frac{l(F+F_s)}{\Gamma D}\right]=-ls(\omega)+\frac{D\Gamma F_s}{F(F+F_s)}, \tag{53}$$

which originates from the expression for the unperturbed equilibrium mean position. For $F<0$, the force F_s is positive, i.e., it acts against the original unperturbed force.

On the whole, the input with vanishing time average generates an effective temperature and frequency-dependent force. The explanation of the effect is simple. The additional energy comes from the external system which creates the driving. It is only due to the absence of a global equilibrium that a part of this energy is constrained within the diffusing system and prevented from being dissipated in the reservoir.

IV. CONCLUDING REMARKS

In the present paper, the external driving of a diffusing particle has been mimicked by a special device which still allows for an exact analysis and which reflects all the pertinent aspects of the dynamics. We have introduced a schematic potential which is modulated at a given point by a step of a time-dependent height. Differently speaking, the diffusing particle encounters at the given point a semipermeable boundary with externally controlled time-dependent permeability.

Having assumed the sudden jump of the potential at the point $x=s$, the force in Eq. (1) exhibits a δ-function singularity. One encounters the well-known problem with an interpretation of the product $\delta(x-s)G(x,y;t)$ [23]. Our way of treating the potential step is effectively equivalent to accepting the Stratonovich interpretation of the above product. Differently speaking, the step is considered as a limiting case of a *continuous* potential which undergoes an abrupt change in the domain $(s-\Delta,s+\Delta)$. The limit $\Delta\to 0$ is implicitly assumed as being the last limit in the calculations.

The analysis of our specific examples has been based on exactly solvable linear potentials. However, the method itself has been developed in a general frame. Thus it is possible to combine, e.g., the parabolic potential or a *W*-shaped profile with the device of time-dependent jumps. The built-in asymmetry of the unperturbed problem has been shown to induce a shift in the time-averaged output signal. A possible application of the result is related with the explanation of the driving-induced shift occurring in ferroelectric systems [24].

As mentioned above, the idea of the time-dependent jump of the potential has been pioneered in Refs. [20,21]. In the work in Ref. [21], the authors analyze the time-asymptotic current in a problem with periodic boundary conditions. Using the matching condition in the same spirit as in the present work, they avoid the Laplace-transform method and they concentrate directly on the stationary regime. At the same time, they invoke the perturbation-like treatment of the jump-modulation amplitude. The present calculation confirms several important features of the results in Ref. [21]. For example, the time-asymptotic characteristics of the diffusion dynamics are necessarily of form (41), i.e., they must contain a fundamental frequency and its higher harmonics. Second, the external frequency enters the results only through the combination $\sqrt{(\omega/D)}$. However, besides a possibility to analyze the transient effects (which is usually not so important), we feel that the present analysis is capable of a more detailed treatment of the harmonics amplitudes and phase shifts. Moreover, the Fourier analysis of the numerical solution of the integral equation yields the exact values of these quantities. This feature could be quite important in the strong-driving regime, when, e.g., the direction of the time-averaged asymptotic current can display counterintuitive

properties and a nontrivial temperature dependence.

An interesting issue connected with our asymmetric problems would be an attempt to find the exact solution of the occurring Volterra integral equation. The full characterization of the resonance effects would necessitate the spectral analysis of the output signal, i.e., the calculation of the signal-to-noise ratio, of the spectral power amplification, etc. One can also focus on the two-time correlation function of the particle's position whose Fourier transform yields the output power spectrum. Within our setting, all these quantities are accessible and calculations are in progress.

In summary, our analysis of the physically transparent and exactly treatable examples evidences again the constructive role played by the noise in the nonlinear dynamics of driven systems.

ACKNOWLEDGMENTS

Support of this work by the Grant Agency of the Czech Republic (Project No. 202/03/0551) and by the Deutsche Forschungsgemeinschaft (Sonderforschungsbereich 569) is gratefully acknowledged. P.Ch. would like to express his gratitude for the warm hospitality extended to him at the Department of Theoretical Physics, University Ulm. We thank Harry L. Frisch and Michael Schulz for useful discussions.

[1] N. G. van Kampen, *Stochastic Processes in Physics and Chemistry* (North-Holland, Amsterdam, 1992).
[2] C. W. Gardiner, *Handbook of Stochastic Methods*, 2nd ed. (Springer, New York, 1985).
[3] H. Risken, *The Fokker-Planck Equation* (Springer, New York, 1989).
[4] P. Reimann and P. Hőnggi, in *Stochastic Dynamics*, edited by L. Schimansky-Geier and T. Pőschel (Springer, Berlin, 1997), pp. 127–139.
[5] R.D. Astumian and M. Bier, Biophys. J. **70**, 637 (1996).
[6] V. S. Anishchenko, V. V. Astakhov, A. B. Neiman, T. E. Vadivasova, and L. Schimansky-Geier, *Nonlinear Dynamics of Chaotic and Stochastic Systems*, Tutorial and Modern Developments, Springer Series in Synergetics (Springer, New York, 2002).
[7] L. Gammaitoni, P. Hőnggi, P. Jung, and F. Marchesoni, Rev. Mod. Phys. **70**, 223 (1998).
[8] P. Reimann, Phys. Rep. **361**, 57 (2002).
[9] M. Mőrsch, H. Risken, and H.D. Vollmer, Z. Phys. B: Condens. Matter **32**, 245 (1979).
[10] H.L. Frisch, V. Privman, C. Nicolis, and D. Nicolis, J. Phys. A **94**, L1147 (1990).
[11] V. Privman, and H.L. Frisch, J. Chem. Phys. **94**, 8216 (1991).
[12] V. Berdichevsky and M. Gitterman, J. Phys. A **29**, 1567 (1996).
[13] Hu Gang, G. Nicolis, and C. Nicolis, Phys. Rev. A **42**, 2030 (1990).
[14] A.K. Dhara and T. Mukhopadhyay, Phys. Rev. E **60**, 2727 (1999).
[15] J. Maddox, Nature (London) **359**, 771 (1992).
[16] C.R. Doering and J.C. Gadoua, Phys. Rev. Lett. **69**, 2318 (1992).
[17] M. Bier and R.D. Astumian, Phys. Rev. Lett. **71**, 1649 (1993).
[18] U. Zürcher and Ch.R. Doering, Phys. Rev. E **47**, 3862 (1993).
[19] T. Novotný and P. Chvosta, Phys. Rev. E **63**, 012102 (2001).
[20] V. Berdichevsky and M. Gitterman, Phys. Rev. E **59**, R9 (1999).
[21] V. Berdichevsky and M. Gitterman, Phys. Rev. E **60**, 7562 (1999).
[22] G. Doetsch, *Anleitung zum praktischen Gebrauch der Laplace-Transformation und der Z-Transformation* (R. Oldenbourg, München, 1967).
[23] C. Van den Broeck, in *Stochastic Dynamics*, edited by L. Schimansky-Geier and T. Pőschel (Springer, Berlin, 1997), pp. 7–14.
[24] A. Përez-Madrid and J.M. Rubí, Phys. Rev. E **51**, 4159 (1995).